

# The Efficiency of Metabolic Labeling of DNA by Diels–Alder Reactions with Inverse Electron Demand: Correlation with the Size of Modified 2′-Deoxyuridines

Dorothee Ganz, Philipp Geng, and Hans-Achim Wagenknecht\*



Cite This: <https://doi.org/10.1021/acschembio.3c00079>



Read Online

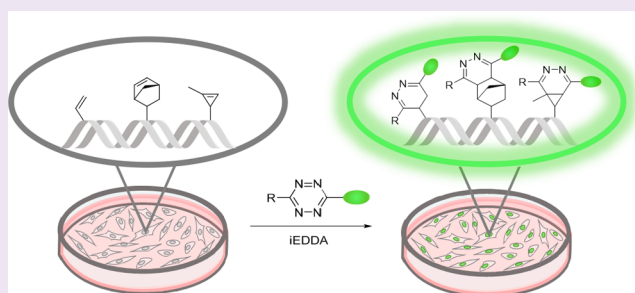
ACCESS |

Metrics & More

Article Recommendations

Supporting Information

**ABSTRACT:** A selection of four different 2′-deoxyuridines with three different dienophiles of different sizes was synthesized. Their inverse electron demand Diels–Alder reactivity increases from  $k_2 = 0.15 \times 10^{-2} \text{ M}^{-1} \text{ s}^{-1}$  to  $k_2 = 105 \times 10^{-2} \text{ M}^{-1} \text{ s}^{-1}$  with increasing ring strain of the dienophiles. With a fluorogenic tetrazine-styryl dye as reactive counterpart the fluorescence turn-on ratios lie in the range of 21–48 suitable for wash-free cellular imaging. The metabolic DNA labeling was visualized by a dot blot on a semiquantitative level and by confocal fluorescence microscopy on a qualitative level. A clear correlation between the steric demand of the dienophiles and the incorporation efficiency of the modified 2′-deoxyuridines into cellular DNA was observed. Even 2′-deoxyuridines with larger dienophiles, such as norbornene and cyclopropene, were incorporated to a detectable level into the nascent genomic DNA. This was achieved by an optimized way of cell culturing. This expands the toolbox of modified nucleosides for metabolic labeling of nucleic acids in general.



Metabolic labeling in combination with bioorthogonal chemistry is an efficient tool for visualization of biomolecules *in vivo*.<sup>1</sup> To gain more understanding of cellular processes, metabolic labeling was initially applied for proteins and glycostructures on the cell surface<sup>2</sup> and extended to an orthogonal approach with two or three fluorescence colors.<sup>3</sup> More recently, metabolic labeling was also applied for imaging nucleic acids inside the cell.<sup>4</sup> Nucleosides modified with a bioorthogonally reactive group are required, which are taken up by the cell and converted into their respective triphosphates by the endogenous enzyme machinery and finally incorporated into nascent nucleic acids by the DNA or RNA polymerases.<sup>5</sup> In combination with bioorthogonal reactions, the modified DNA or RNA can be subsequently labeled and visualized in the cellular environment using bioorthogonal reactions, in particular, the copper-catalyzed<sup>6–10</sup> or strain-promoted azide–alkyne cycloadditions,<sup>11</sup> the “photoclick” reactions,<sup>12,13</sup> and the inverse electron-demand Diels–Alder (iEDDA)<sup>14,15</sup> reactions are used. The iEDDA reaction is the most powerful one due to its intrinsic low toxicity (because metal catalysts are avoided) and fast kinetics.<sup>16</sup>

For DNA and RNA metabolic labeling, nucleosides modified with the vinyl function were used.<sup>13,17,18</sup> Its small size should guarantee and promote the acceptance of the modified nucleosides by the kinases involved in the endogenous phosphorylation process to its triphosphate as building block.<sup>19</sup> However, the vinyl moiety is the simplest dienophile,

and 5-vinyl-2′-deoxyuridine (**1**) yields merely very low second-order reaction rate constants with commercially available tetrazines ( $k_2 = 2.1 \times 10^{-2} \text{ M}^{-1} \text{ s}^{-1}$ ).<sup>15</sup> Despite this disadvantage, Luedtke and co-workers were able to successfully perform metabolic labeling of DNA by using a DNA-intercalating tetrazine-dye conjugate as reaction partner.<sup>20</sup> It would be very useful to introduce more reactive dienophiles into the DNA by means of metabolic labeling to get similar reactivity with a reduced amount of the tetrazine as reacting counterpart, which is important for wash-free imaging of cells. In combination with the concept of fluorogenicity of tetrazine-modified dyes,<sup>21–24</sup> this approach should reduce the background fluorescence with the perspective to gain even better insights into the dynamic processes of DNA inside the cells. Reactive dienophiles for the iEDDA reactions need ring strain and are thus larger than the vinyl group. Such modified 2′-deoxynucleosides might not be accepted by the highly substrate-specific monophosphate kinases or even block the entire enzyme cascade to the respective modified nucleoside triphosphates. Unexpectedly based on this thought, one of the

Received: February 6, 2023

Accepted: February 27, 2023

largest dienophiles, *trans*-cyclooctene, has already been incorporated into RNA by metabolic labeling.<sup>14</sup> However, a systematic study of how the size and reactivity of the dienophile correlate with the efficiency of metabolic labeling is elusive. Herein, we present such a systematic investigation using the synthetic derivatives of 2-deoxyuridine (dU) 2–5 modified with dienophiles with different ring structures, sizes, and reactivities (Figure 1). Their experimental comparison

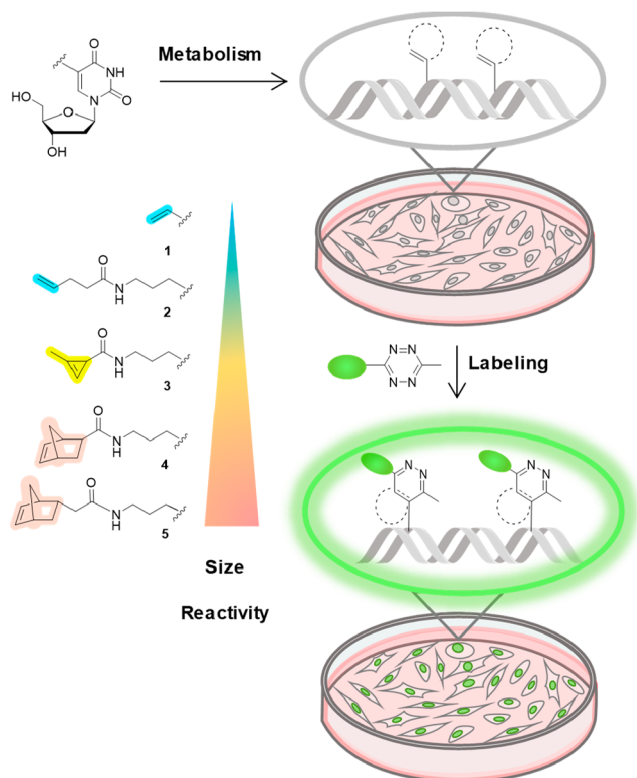


**Figure 1.** 5-Vinyl-2'-deoxyuridine (1) and the synthetically modified 2'-deoxyuridines 2–5 with different dienophiles to correlate their size and kinetics *in vitro* with the efficiency of incorporation by metabolic DNA labeling by a tetrazine-modified dye using the iEDDA reaction *in cellulo*.

should allow us to correlate the size of the dienophile and their kinetics *in vitro* with the efficiency of incorporation by metabolic DNA labeling using the iEDDA reaction *in cellulo*.

To investigate the metabolic incorporation of nucleosides with larger modifications, we synthesized a selection of four different 2'-deoxyuridines 2–5 with three different dienophiles. In all four nucleosides the dienophile is linked to the position C5 of the 2'-deoxynucleoside by the flexible aminopropyl linker that should enable better accessibility for the tetrazine-modified dye 6 for the iEDDA reaction in the densely packed chromatin structure of the genomic DNA. The dienophiles were attached via amide bonds to the 5-(3-aminopropyl)-2'-deoxyuridine as core structure and literature-known synthetic precursor. Nucleoside 2 contains the homallyl, 3 the cyclopropenyl, and 4 and 5 the norbornenyl group as dienophile. In this order, the dienophiles show increasing ring strain and should show increasing reactivity but also increasing steric demand. The complete synthetic procedures are described in the Supporting Information (Scheme S1, Figures S8–S19).

For the kinetic investigations *in vitro*, a tetrazine-modified cyanine-styryl dye (6) developed by our group, which is structurally based on our previously published photostable dyes,<sup>25</sup> was applied because it provides a two-factor fluorogenicity with DNA.<sup>26</sup> The fluorescence of 6 is nearly completely quenched due to the attached tetrazine as quencher moiety.<sup>22,24,26,27</sup> The fluorogenic reaction with the dienophiles in the 2'-deoxyuridines 1–5 converts the quenching tetrazine into the nonquenching diazine (Figure 2). Additionally, the fluorescence is enhanced upon DNA binding due to restricted rotation around the bridging carbon–carbon bonds in the center of the cyanine-styryl dye. This structural fluorogenicity is similar to that of thiazole orange derivatives.<sup>28</sup> The resulting turn-on effect together with the high photostability and the large Stokes shift of 0.50–0.52 eV (95–99 nm) are optimal for fluorescence microscopy. The second-order rate constant, the Stokes shift, and the turn-on effect were determined for the reaction of 1–5 with 6 simply by time-dependent measurements of the fluorescence (Table 1). Since iEDDA reactions are known to have a much higher reaction rate in aqueous solvents<sup>29</sup> and the subsequent application will be in the cellular environment, these reactions were performed in a mixture of H<sub>2</sub>O/dimethyl sulfoxide (DMSO) (99:1 v/v%). The small amount of DMSO is necessary to ensure solubility of all components. The iEDDA reactions were measured over 7 days to ensure complete conversion. The pyridazine products 7–11 were confirmed by electrospray ionization (ESI) mass spectrometry (Table S1 and Figures S20–S24). We assume that the prolonged reaction time in the presence of oxygen yields the pyridazine, except the product 9. The methyl group blocks the dehydrogenation of the dihydropyridazine 9. The rate constants  $k_2$  are relatively low for the reaction of 1–4 with 6 and lie in the range between  $k_2 = 0.15 \times 10^{-2} \text{ M}^{-1} \text{ s}^{-1}$  and  $k_2 = 7.7 \times 10^{-2} \text{ M}^{-1} \text{ s}^{-1}$ . The rate constant for the reaction between 1 and 6 fits reasonably well with the reported  $k_2 = 2.1 \times 10^{-2} \text{ M}^{-1} \text{ s}^{-1}$  in the literature.<sup>15</sup> The measured reaction rates are comparable to reaction rates of SPAAC reactions ( $k_2 \approx 10^{-2} \text{ M}^{-1} \text{ s}^{-1}$ ).<sup>30</sup> In contrast, the reaction between 5 and 6 shows a significantly higher rate constant of  $k_2 = 105 \times 10^{-2} \text{ M}^{-1} \text{ s}^{-1}$ . Faster kinetics were reported in literature only with the highly reactive 3,6-di-2-pyridyl-1,2,4,5-tetrazine or similarly reactive tetrazines.<sup>31,32</sup> Since we want to use these iEDDA reactions specifically for metabolic labeling, those tetrazines are not the right choice for wash-free imaging of cells because they are not fluorogenic. Due to its fluorogenicity, metabolic labeling can be accelerated inside cells by a vast excess of the tetrazine-modified dye 6 (*vide infra*).

Overall, this kinetic and photophysical analysis of the iEDDA reactions between nucleosides 1–5 and tetrazine 6 highlights the reactivity spectrum of these reagents. It expectedly became evident that the dienophiles with higher ring strain, the norbornene in 5, show significantly faster reactions making them promising nucleosides to visualize DNA by labeling *in cellulo*. The fluorescence properties ( $\lambda_{em}$  and Stokes shift) of the products 7–11 are very similar and do not depend on the different structures of the linkers between the dye and the dU moiety. The fluorescence turn-on observed during the reactions of 1 and 3–5 with the tetrazine-modified dye 6 is quite similar; the values lie in the range between 21 and 25 and are suitable for cellular imaging. The fluorescence turn-on is higher for the reaction with 2, which might be attributed to the longer and thus more flexible alkyl linker.

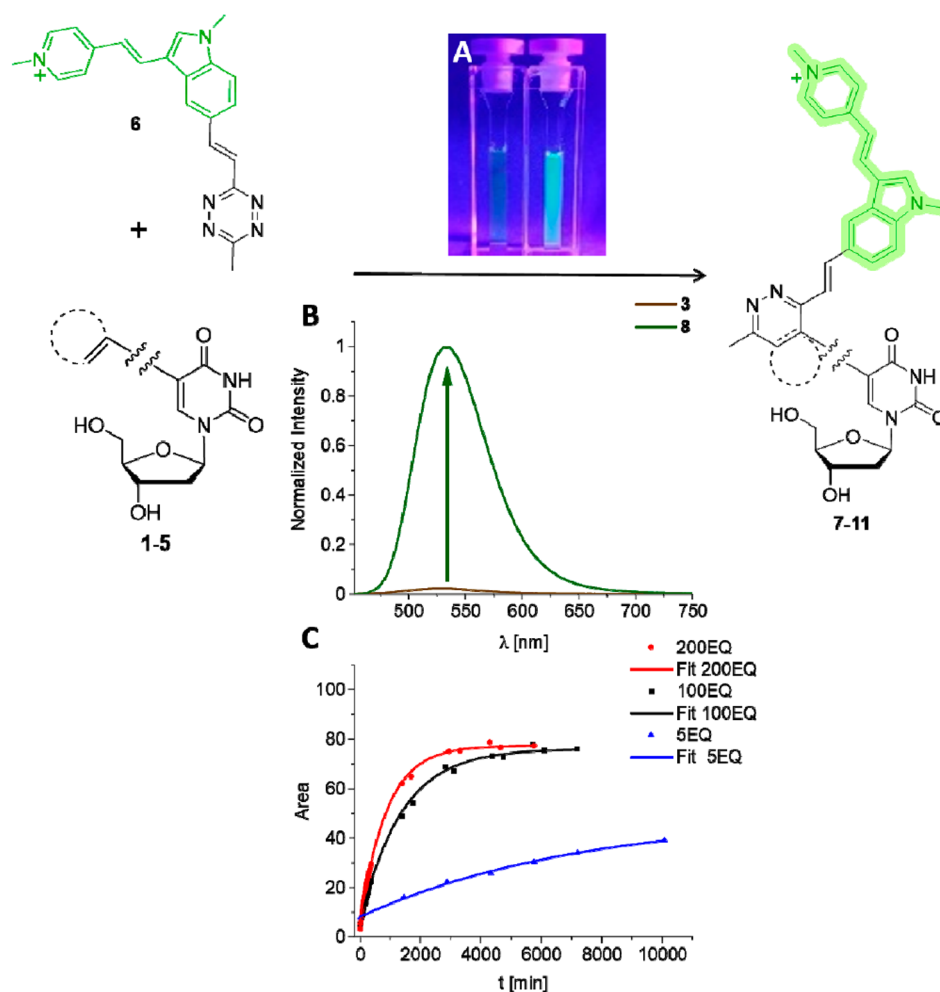


**Figure 2.** iEDDA reaction of the 2'-deoxyuridines 1–5 and the tetrazine-modified dye 6 to the “clicked” products 7–11. (A) Visible turn-on effect; left: 20  $\mu\text{M}$  6 before the iEDDA reaction; right: after reaction with 3. (B) Increase in fluorescence intensity ( $\lambda_{\text{ex}} = 437 \text{ nm}$ ) observed for the reaction of 3 (5, 200, 200 equiv) with 6 (20  $\mu\text{M}$ ) in  $\text{H}_2\text{O}$  (with 1% DMSO). (C) Concentration-dependent kinetic plots of the “click” reaction of 6 + 3 with exponential fit functions:  $y = a + b \cdot \exp(-k \cdot x)$ . For the results with 1, 2, 4, and 5 see [Supporting Information](#) (Figures S1–S5).

**Table 1. Second-Order Rate Constants and Photophysical Properties for the iEDDA Reaction of the 2'-Deoxyuridines (dU) 1–5 with the Tetrazine-Modified Dye 6 to the Products 7–11 in  $\text{H}_2\text{O}/\text{DMSO}$  (99:1 v/v)**

dU	product	$\lambda_{\text{em}}$ [nm]	$\Delta\lambda$ [eV] <sup>a</sup>	$\Delta\lambda$ [nm] <sup>a</sup>	Turn-on	$\Phi_{\text{F}}$ <sup>b</sup>	$k_2 \cdot 10^{-2} [\text{M}^{-1} \text{s}^{-1}]$
1	7	536	0.524	99	21	0.012	$0.37 \pm 0.01$
2	8	534	0.515	97	48	0.019	$0.15 \pm 0.01$
3	9	532	0.506	95	23	0.008	$0.51 \pm 0.05$
4	10	535	0.520	98	25	0.010	$7.70 \pm 0.60$
5	11	532	0.506	95	22	0.012	$105 \pm 4.00$

<sup>a</sup>Stokes shift. <sup>b</sup>Quantum yield measured in  $\text{H}_2\text{O}/\text{DMSO}$  (99:1).

To evaluate the metabolic incorporation of nucleosides 2–5 into cellular DNA, we first examined their cellular toxicity. The cell viability was determined by using the 3-(4,5-dimethylthiazol-2-yl)-2,5-diphenyltetrazolium bromide (MTT) assay (Figure S6). The determination of the median lethal dose (LD50) is as much as 0.3 mM for all nucleosides. Thus, the nucleosides are not toxic under the conditions applied (250  $\mu\text{M}$ ). The nucleosides 3 and 4 show toxicity in concentrations of at least 0.5 mM.

It is known that the monophosphate nucleoside kinases involved in the nucleoside metabolic pathway have the highest specificity for their substrates within the metabolism from nucleoside to DNA.<sup>19</sup> Therefore, it was often assumed that long linkers and larger structures such as norbornene or cyclopropene are not accepted by the kinases or even result in the inhibition of this metabolic pathway. The acceptance of a longer linker system by which the dienophile is connected to the nucleoside has already been demonstrated by Tang *et al.*<sup>33</sup> Furthermore, Zhou's group modified an adenosine at the position N6 with a 1,3-dimethylcycloprop-1-ene, which was successfully used for the metabolic labeling of RNA.<sup>34</sup> Both studies demonstrated that such larger modifications of nucleosides might be accepted and metabolized by the cell.

The modified nucleosides 2–5 were not sufficiently metabolically incorporated into the DNA of HeLa cells using the conventional Dulbecco's Modified Eagle's Medium (DMEM, Figure S9). In order to force the cells to incorporate the modified 2'-deoxyuridines 2–5 as substitutes for thymidine by their metabolism and to overcome the problem with the nucleotide kinase selectivity, we worked out new and optimized cell culture conditions. HeLa cells were cultured in a minimum essential medium (MEM- $\alpha$ ) without L-

glutamine, supplemented with 10% dialyzed fetal calf serum and 1% penicillin and streptomycin, instead of the conventional DMEM. L-Glutamine is an essential nitrogen source for the metabolic nucleoside synthesis.<sup>35</sup> To diminish the competition between modified and natural nucleosides, the cells should be cultured in a medium with the natural nucleosides excluding T (for the dot blot analysis) and without any of the natural nucleosides (for confocal microscopy). This should increase the incorporation of the modified nucleosides by artificially decreasing the natural building blocks. The 2'-deoxyuridines 2–5 were added to the culture medium from 1 M stock solutions with a final concentration of 250  $\mu$ M and less than 1% DMSO. To demonstrate the incorporation of the modified 2'-deoxynucleosides 2–5 into nascent DNA we first performed biotinylation of isolated DNA via the iEDDA reaction with a commercially available biotin-tetrazine conjugate. Subsequently, we used a horseradish peroxidase (HRP)-streptavidin dot blot to detect the presence of the nucleosides on a semiquantitative level (Figure 3).<sup>17</sup> The

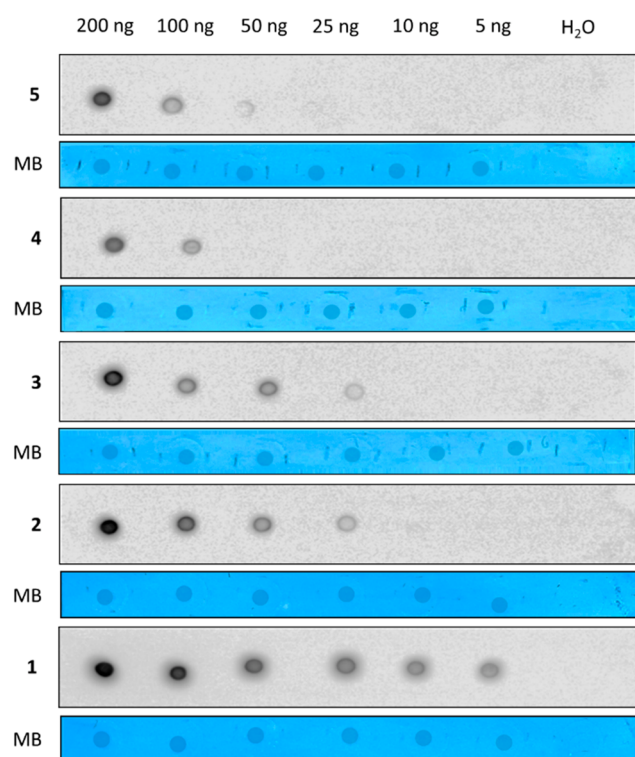


**Figure 3.** Images of HRP-streptavidin dot blots of isolated DNA after metabolic labeling with 1–5 (incubation with 250  $\mu$ M for 72 h) verifies the successful incorporation of the reactive labels into cellular DNA. Gray spots: Marking with a commercially available biotin-tetrazine conjugate, incubation with HRP-streptavidin and imaging by chemiluminescence. Blue spots: Total DNA spotted onto each membrane was controlled with methylene blue (MB) staining.

genomic DNA was isolated, and 15  $\mu$ g of the isolated DNA was incubated with 1 mM of the tetrazine-biotin conjugate for 24 h at 37  $^{\circ}$ C and then eluted. For dot blotting, different concentrations (200–5 ng) of biotinylated DNA were spotted. After UV cross-linking of the DNA to the membrane and incubation with HRP-streptavidin, the dot blot was imaged by chemiluminescence. In a final step, the membrane was stained by methylene blue solution to make the spotted DNA visible. The results of this dot blot revealed a significant and

remarkable dependence of the size and steric demand of the dienophile on the incorporation efficiency into the DNA. While the DNA labeled by the norbornene (using 4 and 5) can only be detected in the highest concentrations (200–50 ng), the DNA with the cyclopropane (using 3) and the vinyl (using 2) labels can also be detected at lower concentrations (25 ng), which clearly evidence the higher incorporation efficiency of the latter 2'-deoxynucleosides due to their smaller dienophiles. The smallest nucleoside 1 is detectable down to 5 ng DNA on the blot. It is important to underscore here that—although spatially demanding dienophiles have a lower efficiency of incorporation—they are *all* accepted to a certain extent by the nucleoside metabolism of the cell, transferred through the metabolic pathway, and thus successfully incorporated into nascent DNA.

Based on these results, we were encouraged to finally apply the 2'-deoxyuridines 2–5 for metabolic DNA labeling and imaging by means of the iEDDA reaction with 6 in cells under wash-free conditions. HeLa cells were incubated for 24 h with 250  $\mu$ M of each of the nucleosides 2–5 using again the cell culture conditions mentioned above. Cells were then fixed with paraformaldehyde. Without prior denaturation of the DNA, fluorescent labeling was performed with 20  $\mu$ M of 6 for 24 h. Without any further washing step, the DNA labeling in the cell nuclei could be visualized under a confocal fluorescence microscope using an excitation wavelength of 488 nm (Figure 4). Cells treated without a modified nucleoside served as a negative control to demonstrate the very low background fluorescence of unreacted dye 6. As an additional control, a counterstain was performed with Hoechst (Figure S7), which matched the fluorescent signals obtained from the iEDDA reaction. Additionally, we observed staining of the mitochondrial DNA and of remaining 2'-deoxyuridine in the cytosol due to the wash-free method, which is most obvious for 2. This was not observed to such an extent with nucleosides 3–5, which is an advantage of these nucleosides. The fluorescent imaging of the cells confirmed the correlation between the size of the dienophile and the incorporation of the corresponding 2'-deoxyuridine into the genomic DNA that we already obtained by the dot blot. The norbornene-modified nucleosides 4 and 5 showed a significantly weaker fluorescence signal than the smaller modifications of the cyclopropane (3) and the vinyl function (2), as this was also seen in the dot blot. Despite these differences, it is important to mention that all modified 2'-deoxyuridines gave enough fluorescent DNA labeling products by the metabolic pathway and provided a sufficiently strong fluorescence signal to visualize the cellular DNA in the cellular environment without prior denaturation of the DNA.

In conclusion, we provide for the first time a systematic study of how the size of the dienophile-modified 2'-deoxynucleoside influences the efficiency of metabolic labeling of cellular DNA by means of the iEDDA reaction. We synthesized a selection of four different 2'-deoxyuridines 2–5 with three different dienophiles of different sizes and combined them with the concept of fluorogenicity using the tetrazine-modified cyanine-styryl dye 6. Expectedly, the reactivity increases from  $k_2 = 0.15 \times 10^{-2} \text{ M}^{-1} \text{ s}^{-1}$  for 2 to  $k_2 = 105 \times 10^{-2} \text{ M}^{-1} \text{ s}^{-1}$  for 5. The fluorescence turn-on ratios lie in the range between 21 and 48 and are suitable for cellular imaging without any washing. The metabolic DNA labeling was visualized by the dot blot on a semiquantitative level and by confocal microscopy on a qualitative level. A clear correlation between the size and steric demand of the dienophiles and the

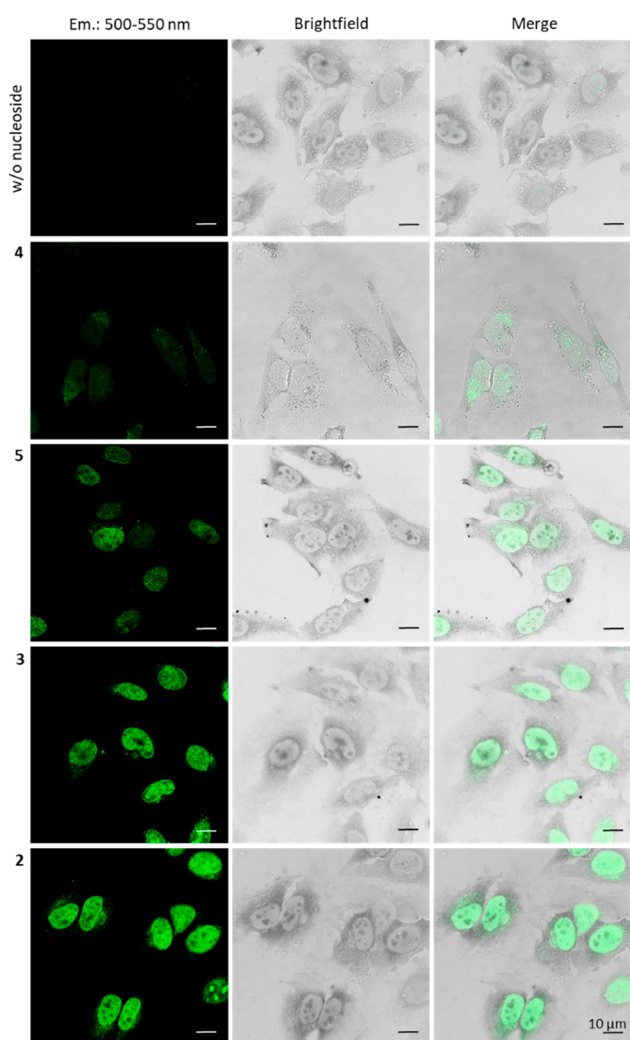


**Figure 4.** HeLa cells were incubated for 24 h with nucleosides 2–5 (250  $\mu\text{M}$ ) for 24 h. Cells were then fixed with paraformaldehyde. Without prior denaturation, the DNA was labeled with the tetrazine-dye **6** (20  $\mu\text{M}$ ) for 24 h. Imaging via confocal fluorescence microscopy with a 488 nm laser line and a fluorescence emission channel at 500–550 nm, complemented with a brightfield channel. Cells treated without any modified 2'-deoxynucleoside served as a negative control. Scale bar: 10  $\mu\text{m}$ .

incorporation efficiency of the correspondingly modified 2'-deoxyuridines into cellular DNA was observed. We demonstrated that even 2'-deoxyuridines with larger dienophiles, such as norbornene and cyclopropene, were accepted by the endogenous enzymes of DNA metabolic pathways and incorporated to a detectable level into the nascent genomic DNA of HeLa cells. This was achieved by an optimized way of cell culturing. Taken together these are remarkable results and were not expected based on the literature. That opens new possibilities and broadens the molecular toolbox for metabolic labeling of DNA, because 2'-deoxynucleosides with larger and ring-strained dienophiles that undergo potentially faster iEDDA reactions with dyes than the conventional 5-vinyl-2'-deoxyuridine (**1**), like the norbornene modification in **4**, can also be incorporated. However, the crucial factor for an iEDDA reaction to take place in the densely packed chromatin structure is the accessibility of the two reaction partners. With regard to the tetrazine-modified dyes we used, the two-factor

fluorogenicity provides significant potential to further exploit the iEDDA reaction for DNA and RNA imaging *in cellulo* without denaturation and without washing steps. The DNA-sensitive tetrazine-dye **6** is able to penetrate the densely packed structure of chromatin. A precisely coordinated combination of dienophile and tetrazine can lead to efficient labeling.<sup>20,33</sup> To the best of our knowledge, norbornene- and cyclopropene-modified nucleosides have not yet been used for metabolic labeling of DNA because these dienophiles were always considered as too big. This study complements the known results from literature and thereby provides a deeper understanding. Based on our results, the toolbox of modified nucleosides for metabolic labeling of both DNA and RNA can be further expanded.

## ■ ASSOCIATED CONTENT

### Supporting Information

The Supporting Information is available free of charge at <https://pubs.acs.org/doi/10.1021/acscchembio.3c00079>.

Materials and methods, synthetic procedures, kinetic studies and fluorescence measurements, cell biology methods, images of NMR spectra, and mass spectrometric analyses (PDF)

## ■ AUTHOR INFORMATION

### Corresponding Author

Hans-Achim Wagenknecht – Institute of Organic Chemistry, Karlsruhe Institute of Technology, 76131 Karlsruhe, Germany; [orcid.org/0000-0003-4849-2887](https://orcid.org/0000-0003-4849-2887); Email: [Wagenknecht@kit.edu](mailto:Wagenknecht@kit.edu)

### Authors

Dorothee Ganz – Institute of Organic Chemistry, Karlsruhe Institute of Technology, 76131 Karlsruhe, Germany  
 Philipp Geng – Institute of Organic Chemistry, Karlsruhe Institute of Technology, 76131 Karlsruhe, Germany

Complete contact information is available at:

<https://pubs.acs.org/doi/10.1021/acscchembio.3c00079>

### Author Contributions

The manuscript was written through contributions of all authors. All authors have given approval to the final version of the manuscript.

### Funding

Deutsche Forschungsgemeinschaft (grants Wa-1386/17-2, Wa-1386/22-1, and GRK 2039/2).

### Notes

The authors declare no competing financial interest.

## ■ ACKNOWLEDGMENTS

Financial support by the KIT is gratefully acknowledged.

## ■ REFERENCES

- (1) Prescher, J. A.; Bertozzi, C. R. Chemistry in living systems. *Nat. Chem. Biol.* **2005**, *1*, 13–21.
- (2) Hang, H. C.; Bertozzi, C. R. Chemoselective Approaches to Glycoprotein Assembly. *Acc. Chem. Res.* **2001**, *34*, 727–736.
- (3) Niederwieser, A.; Späte, A.-K.; Nguyen, L. D.; Jüngst, C.; Reutter, W.; Wittmann, V. Two-Color Glycan Labeling of Live Cells by a Combination of Diels-Alder and Click Chemistry. *Angew. Chem., Int. Ed.* **2013**, *52*, 4265–4268.

- (4) Gupta, M.; Levine, S. R.; Spitale, R. C. Probing Nascent RNA with Metabolic Incorporation of Modified Nucleosides. *Acc. Chem. Res.* **2022**, *55*, 2647–2659.
- (5) Ganz, D.; Harijan, D.; Wagenknecht, H.-A. Labelling of DNA and RNA in the cellular environment by means of bioorthogonal chemistry. *RSC Chem. Biol.* **2020**, *1*, 86–97.
- (6) Zajackowski, E. L.; Zhao, Q.-Y.; Zhang, Z. H.; Li, X.; Wei, W.; Marshall, P. R.; Leighton, L. J.; Nainar, S.; Feng, C.; Spitale, R. C.; Bredy, T. W. Bioorthogonal Metabolic Labeling of Nascent RNA in Neurons Improves the Sensitivity of Transcriptome-Wide Profiling. *ACS Chem. Neurosci.* **2018**, *9*, 1858–1865.
- (7) Neef, A. B.; Pernot, L.; Schreier, V. N.; Scapozza, L.; Luedtke, N. W. A Bioorthogonal Chemical Reporter of Viral Infection. *Angew. Chem., Int. Ed.* **2015**, *54*, 7911–7914.
- (8) Huynh, N.; Dickson, C.; Zencak, D.; Hilko, D. H.; Mackay-Sim, A.; Poulsen, S.-A. Labeling of Cellular DNA with a Cyclosal Phosphotriester Pronucleotide Analog of 5-ethynyl-2'-deoxyuridine. *Chem. Biol. Drug Des.* **2015**, *86*, 400–409.
- (9) Jao, C. Y.; Salic, A. Exploring RNA transcription and turnover *in vivo* by using click chemistry. *Proc. Natl. Acad. Sci. U.S.A.* **2008**, *105*, 15779–15784.
- (10) Curanovic, D.; Cohen, M.; Singh, I.; Slagle, C. E.; Leslie, C. S.; Jaffrey, S. R. Global profiling of stimulus-induced polyadenylation in cells using a poly(A) trap. *Nature Chem. Biol.* **2013**, *9*, 671–675.
- (11) Tera, M.; Luedtke, N. W. Three-Component Bioorthogonal Reactions on Cellular DNA and RNA. *Bioconjugate Chem.* **2019**, *30*, 2991–2997.
- (12) Nainar, S.; Kubota, M.; McNitt, C.; Tran, C.; Popik, V. V.; Spitale, R. C. Temporal Labeling of Nascent RNA Using Photoclick Chemistry in Live Cells. *J. Am. Chem. Soc.* **2017**, *139*, 8090–8093.
- (13) Wu, Y.; Guo, G.; Zheng, J.; Xing, D.; Zhang, T. Fluorogenic "Photoclick" Labeling and Imaging of DNA with Coumarin-Fused Tetrazole *In Vivo*. *ACS Sens.* **2019**, *4*, 44–51.
- (14) Wu, K.; He, M.; Khan, I.; Asare Okai, P. N.; Lin, Q.; Fuchs, G.; Royzen, M. Bio-orthogonal chemistry-based method for fluorescent labelling of ribosomal RNA in live mammalian cells. *Chem. Commun.* **2019**, *55*, 10456–10459.
- (15) Rieder, U.; Luedtke, N. W. Alkene-Tetrazine Ligation for Imaging Cellular DNA. *Angew. Chem. Int. Ed.* **2014**, *53*, 9168–9172.
- (16) Blackman, M. L.; Royzen, M.; Fox, J. M. Tetrazine Ligation: Fast Bioconjugation Based on Inverse-Electron-Demand Diels-Alder Reactivity. *J. Am. Chem. Soc.* **2008**, *130*, 13518–13519.
- (17) Gupta, M.; Singha, M.; Rasale, D. B.; Zhou, Z.; Bhandari, S.; Beasley, S.; Sakr, J.; Parker, S. M.; Spitale, R. C. Mutually Orthogonal Bioconjugation of Vinyl Nucleosides for RNA Metabolic Labeling. *Org. Lett.* **2021**, *23*, 7183–7187.
- (18) Nguyen, K.; Kubota, M.; del Arco, J.; Feng, C.; Singha, M.; Beasley, S.; Sakr, J.; Gandhi, S. P.; Blurton-Jones, M.; Fernandez Lucas, J.; Spitale, R. C. A Bump-Hole Strategy for Increased Stringency of Cell-Specific Metabolic Labeling of RNA. *ACS Chem. Biol.* **2020**, *15*, 3099–3105.
- (19) Kubota, M.; Nainar, S.; Parker, S. M.; England, W.; Furche, F.; Spitale, R. C. Expanding the Scope of RNA Metabolic Labeling with Vinyl Nucleosides and Inverse Electron-Demand Diels-Alder Chemistry. *ACS Chem. Biol.* **2019**, *14* (8), 1698–1707.
- (20) Loehr, M. O.; Luedtke, N. W. A Kinetic and Fluorogenic Enhancement Strategy for Labeling of Nucleic Acids. *Angew. Chem., Int. Ed.* **2022**, *61*, e202112931.
- (21) Wiczorek, A.; Werther, P.; Euchner, J.; Wombacher, R. Green-to far-red-emitting fluorogenic tetrazine probes - synthetic access and no-wash protein imaging inside living cells. *Chem. Sci.* **2017**, *8*, 1506–1510.
- (22) Devaraj, N. K.; Hilderbrand, S.; Upadhyay, R.; Mazitschek, R.; Weissleder, R. Bioorthogonal Turn-On Probes for Imaging Small Molecules inside Living Cells. *Angew. Chem., Int. Ed.* **2010**, *49*, 2869–2872.
- (23) Kormos, A.; Egyed, A.; Olvany, J. M.; Szatmári, Á.; Biró, A.; Csorba, Z.; Kele, P.; Németh, K. A Bioorthogonal Double Fluorogenic Probe to Visualize Protein-DNA Interaction. *Chemosensors* **2022**, *10*, 37.
- (24) Wu, H.; Devaraj, N. K. Advances in Tetrazine Bioorthogonal Chemistry Driven by the Synthesis of Novel Tetrazines and Dienophiles. *Acc. Chem. Res.* **2018**, *51*, 1249–1259.
- (25) Schwechheimer, C.; Rönicke, F.; Schepers, U.; Wagenknecht, H.-A. A new structure-activity relationship for cyanine dyes to improve photostability and fluorescence properties for live cell imaging. *Chem. Sci.* **2018**, *9*, 6557–6563.
- (26) Geng, P.; List, E.; Rönicke, F.; Wagenknecht, H.-A. Two-Factor Fluorogenicity of Tetrazine-Modified Cyanine-Styryl Dyes for Bioorthogonal Labelling of DNA. *Chem.-Eur. J.* **2023**, DOI: 10.1002/chem.202203156.
- (27) Werther, P.; Yserentant, K.; Braun, F.; Grufmayer, K.; Navikas, V.; Yu, M.; Zhang, Z.; Ziegler, M. J.; Mayer, C.; Gralak, A. J.; Busch, M.; Chi, W.; Rominger, F.; Radenovic, A.; Liu, X.; Lemke, E. A.; Buckup, T.; Hertel, D.-P.; Wombacher, R. Bio-orthogonal Red and Far-Red Fluorogenic Probes for Wash-Free Live-Cell and Super-Resolution Microscopy. *ACS Cent. Sci.* **2021**, *7*, 1561–1571.
- (28) Würthner, F. Aggregation-Induced Emission (AIE): A Historical Perspective. *Angew. Chem., Int. Ed.* **2020**, *59*, 14192–14196.
- (29) Meijer, A.; Otto, S.; Engberts, J. B. F. N. Effects of the Hydrophobicity of the Reactants on Diels–Alder Reactions in Water. *J. Org. Chem.* **1998**, *63* (24), 8989–8994.
- (30) Cserép, G. B.; Herner, A.; Kele, P. Bioorthogonal fluorescent labels: a review on combined forces. *Methods and applications in fluorescence* **2015**, *3* (4), 042001.
- (31) Yang, J.; Liang, Y.; Šečkutė, J.; Houk, K. N.; Devaraj, N. K. Synthesis and Reactivity Comparisons of 1-Methyl-3-Substituted Cyclopropene Mini-tags for Tetrazine Bioorthogonal Reactions. *Chem.-Eur. J.* **2014**, *20* (12), 3365–3375.
- (32) Devaraj, N. K.; Weissleder, R.; Hilderbrand, S. A. Tetrazine-based cycloadditions: application to pretargeted live cell imaging. *Bioconjugate Chem.* **2008**, *19* (12), 2297–9.
- (33) Gubu, A.; Li, L.; Ning, Y.; Zhang, X.; Lee, S.; Feng, M.; Li, Q.; Lei, X.; Jo, K.; Tang, X. Bioorthogonal Metabolic DNA Labelling using Vinyl Thioether-Modified Thymidine and o-Quinolinone Quinone Methide. *Chem.-Eur. J.* **2018**, *24* (22), 5895–5900.
- (34) He, Z.; Peng, S.; Wei, Q.; Jia, S.; Guo, S.; Chen, K.; Zhou, X. Metabolic Labeling and Imaging of Cellular RNA via Bioorthogonal Cyclopropene-Tetrazine Ligation. *CCS Chem.* **2020**, *2* (3), 89–97.
- (35) Pelley, J. W. Purine, Pyrimidine, and Single-Carbon Metabolism. In *Elsevier's Integrated Review Biochemistry*, 2nd ed.; Pelley, J. W., Ed.; W.B. Saunders: Philadelphia, PA, 2012; pp 119–124.